

Supporting Information for

Floating Gate Negative Capacitance MoS₂ Phototransistor with High Photosensitivity

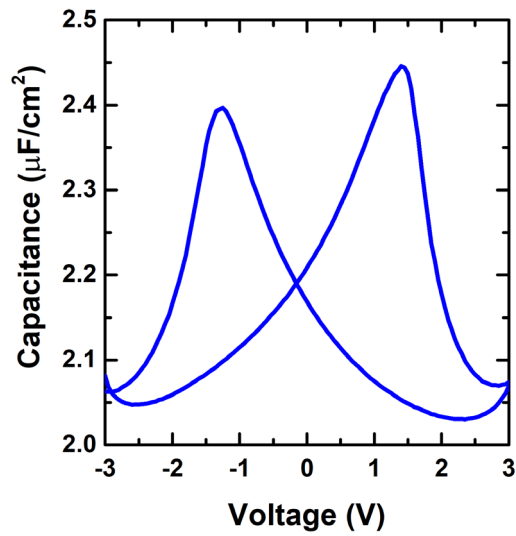
Roda Nur^{1}, Takashi Tsuchiya², Kasidit Toprasertpong¹, Kazuya Terabe², Shinichi*

Takagi¹, and Mitsuru Takenaka¹

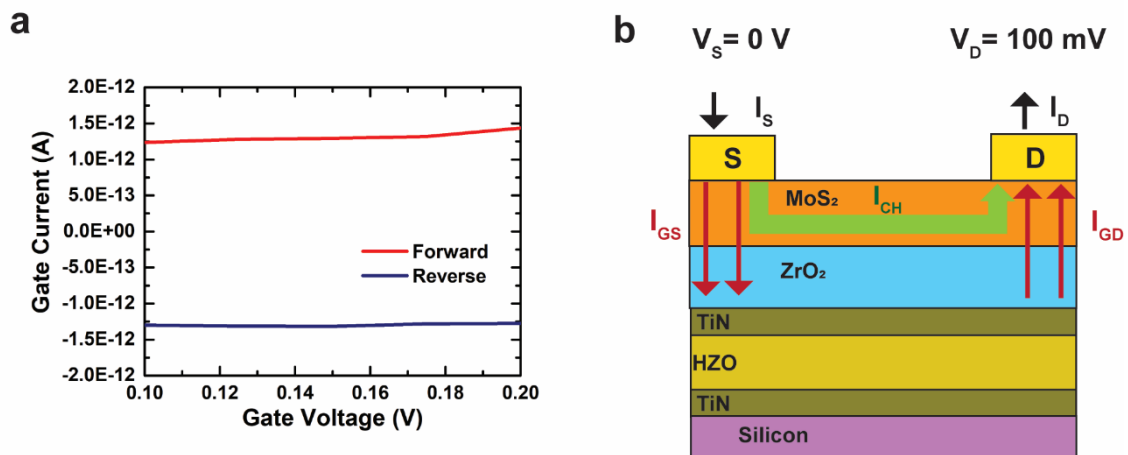
¹Department of Electrical Engineering and Information Systems, The University of
Tokyo, 7-3-1 Hongo, Bunkyo-ku, Tokyo 113-8656, Japan

²International Center for Materials Nanoarchitectonics (WPI-MANA), National Institute
for Materials Science (NIMS), Tsukuba, Ibaraki 305-0044, Japan

*Email: nur@mosfet.t.u-tokyo.ac.jp



Supplementary Figure 1. Capacitance-voltage of MFM at 1kHz.



Supplementary Figure 2. (a) Gate current as a function of the gate voltage. (b) Schematic of current flow in the device.

In the low subthreshold region it is was found that $I_D < I_G$; therefore, reporting SS_{min} in this region can misleading due to the contribution of the gate current to the measured drain current. In order to evaluate SS_{min} , we observed that in the region around $V_G = 0.1$ V, I_G is constant as seen in Supplementary Figure 2a. The total current flow in the device is in Supplementary Figure 2b.

The total currents in this back-gated device^[2] is:

$$I_G = I_{GS} - I_{GD}$$

$$I_D = I_{ch} + I_{GD}$$

$$I_S = I_{ch} + I_{GS}$$

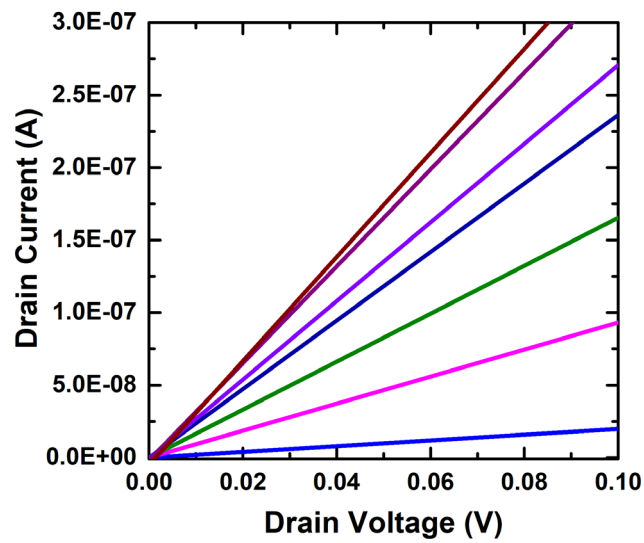
Since $I_G = \text{constant}$, we make an approximation that I_G can be divided into two equal parts where:

$$I_{GS} = 0.5 * I_G$$

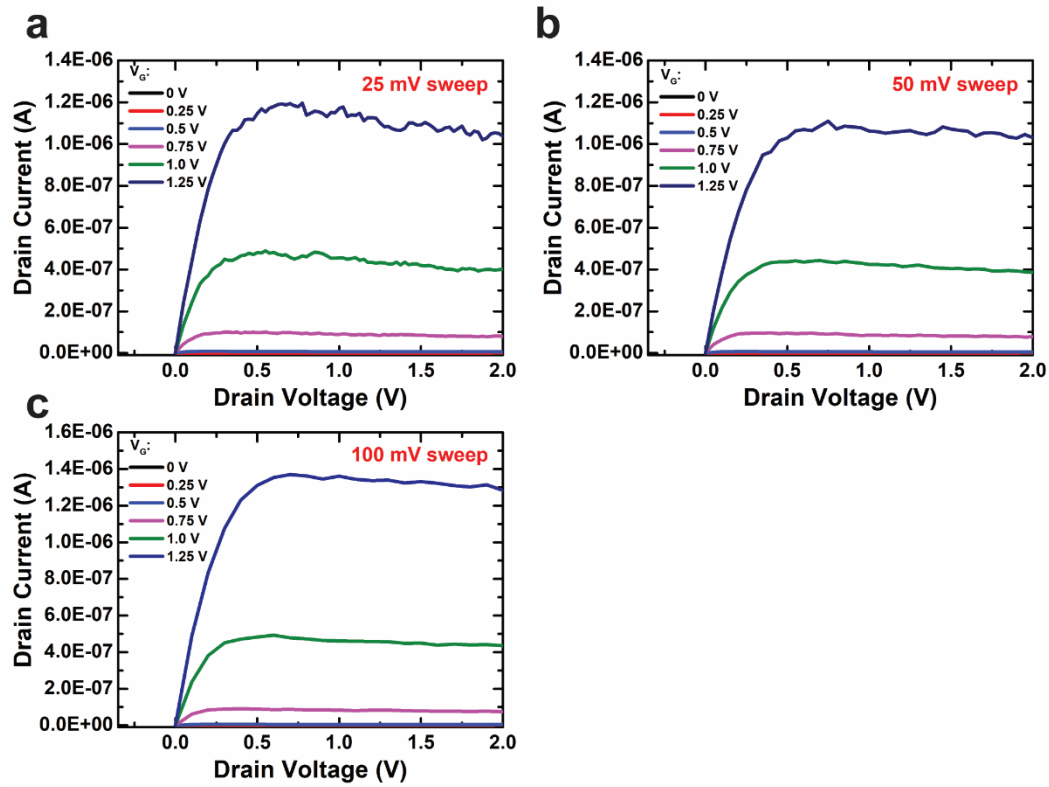
$$I_{GD} = 0.5 * I_G$$

Therefore, the drain current without the contribution of the gate current in this region is determined from:

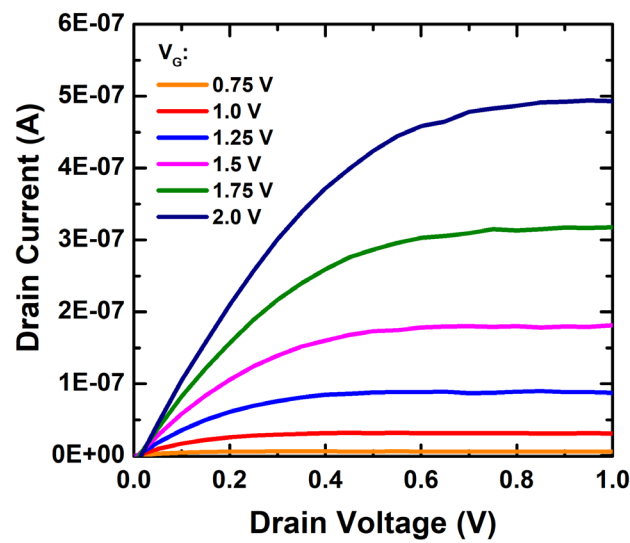
$$I_D = I_{D,\text{measured}} - 0.5 * I_G$$



Supplementary Figure 3. Close up of dark condition I_D - V_D at low drain voltages. The linear curves indicate ohmic-like contacts to monolayer MoS₂.

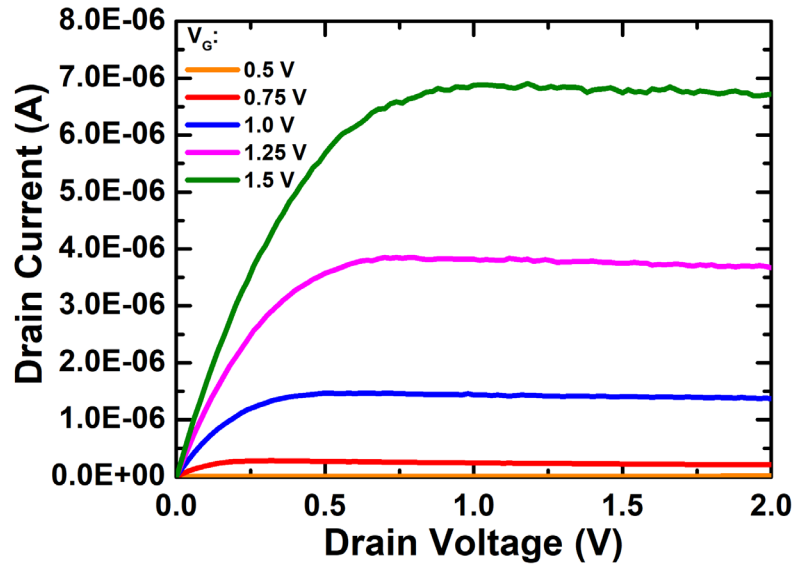


Supplementary Figure 4. Output characteristics of NCFG device with different drain voltage sweeps at (a) 25 mV, (b) 50 mV, and (c) 100 mV. This device measurement is from a different device from the result in the main article.

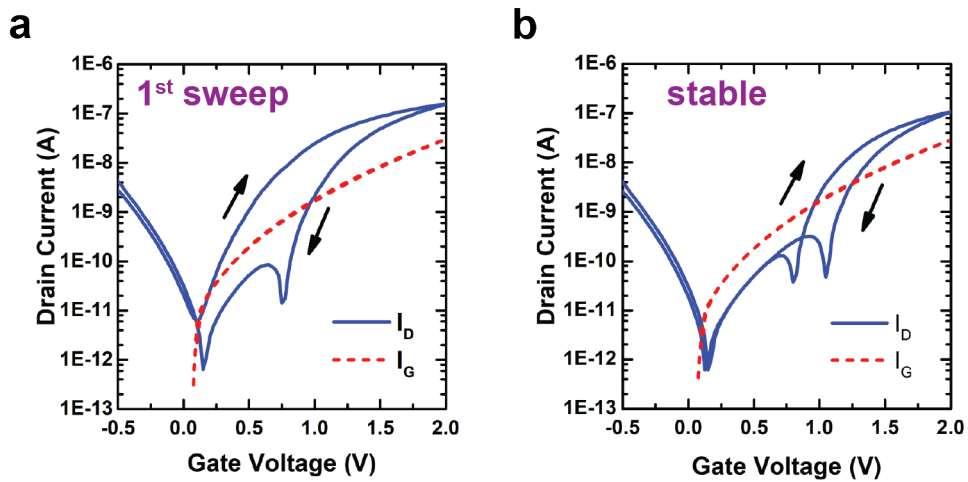


Supplementary Figure 5. Output characteristics of Si/ZrO₂ device under the dark

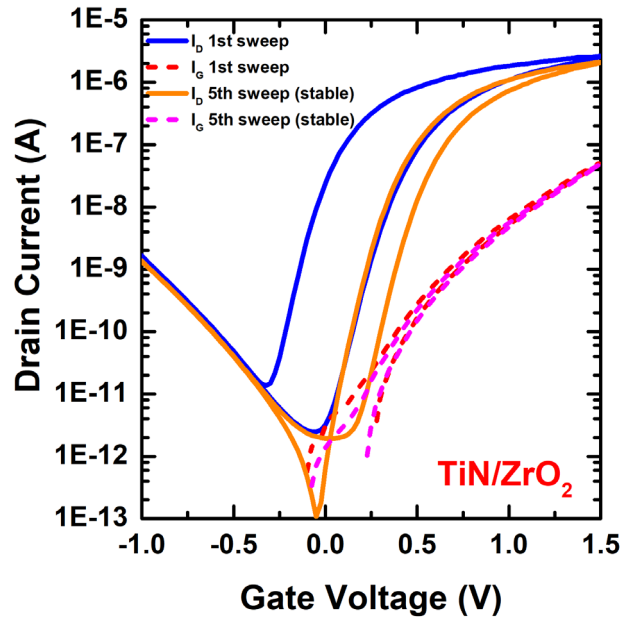
condition.



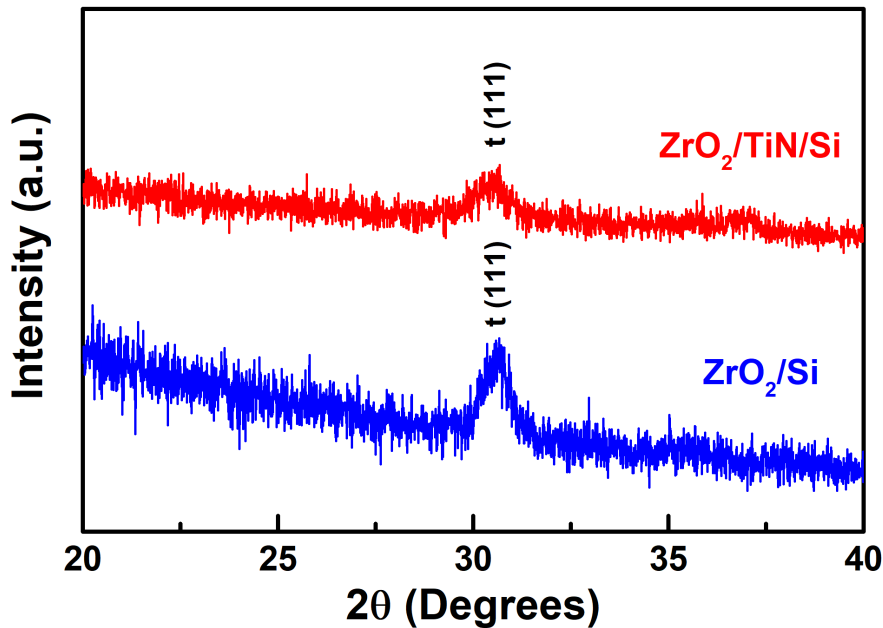
Supplementary Figure 6. Output characteristics of TiN-ZrO₂ device under the dark condition. The drain voltage sweep was at 20 mV.



Supplementary Figure 7. Transfer characteristics of backgated device structure of Si/ZrO₂/MoS₂ with V_{DS} = 150 mV. (a) After first I_D-V_G sweep. (b) After a few I_D-V_G sweeps, the transfer characteristics became stable; however, the I_{on}/I_{off} ratio became lower.

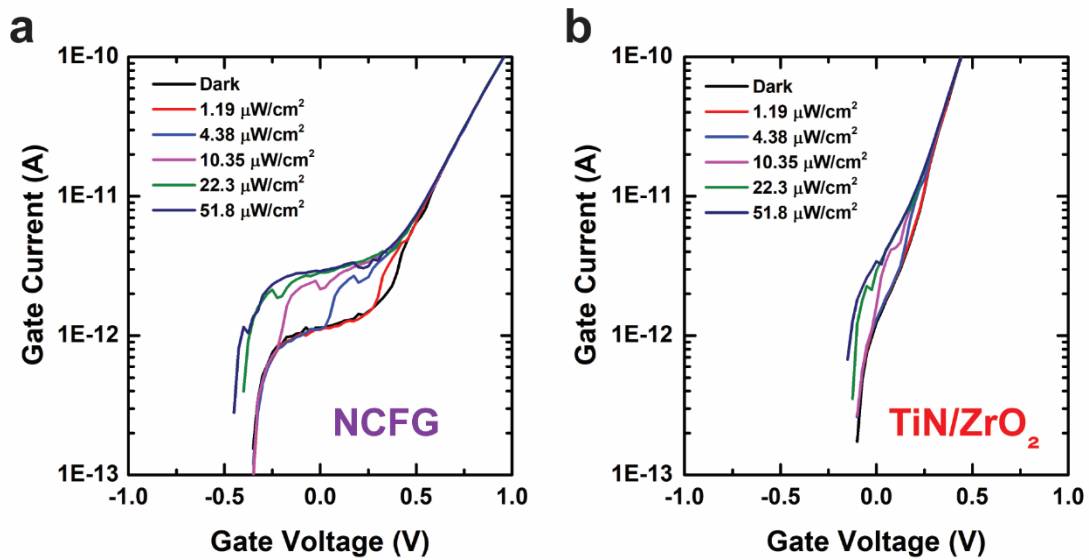


Supplementary Figure 8. Transfer characteristics of backgated device structure of Si/TiN/ZrO₂/MoS₂ including the first sweep and stable sweep.

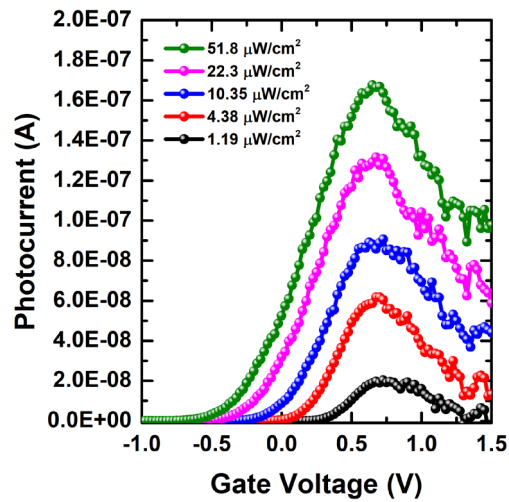


Supplementary Figure 9. XRD of ZrO₂ and TiN/ZrO₂ after ALD deposition at 300 °C with no post deposition annealing. Both films showed a small broad peak corresponding to the tetragonal (111) crystal phase at ~30.4°^[2]; however, the ZrO₂ on Si showed a stronger peak intensity possibly indicating that this crystal growth is more preferable on a silicon interface rather than TiN at this deposition temperature. Overall, this result

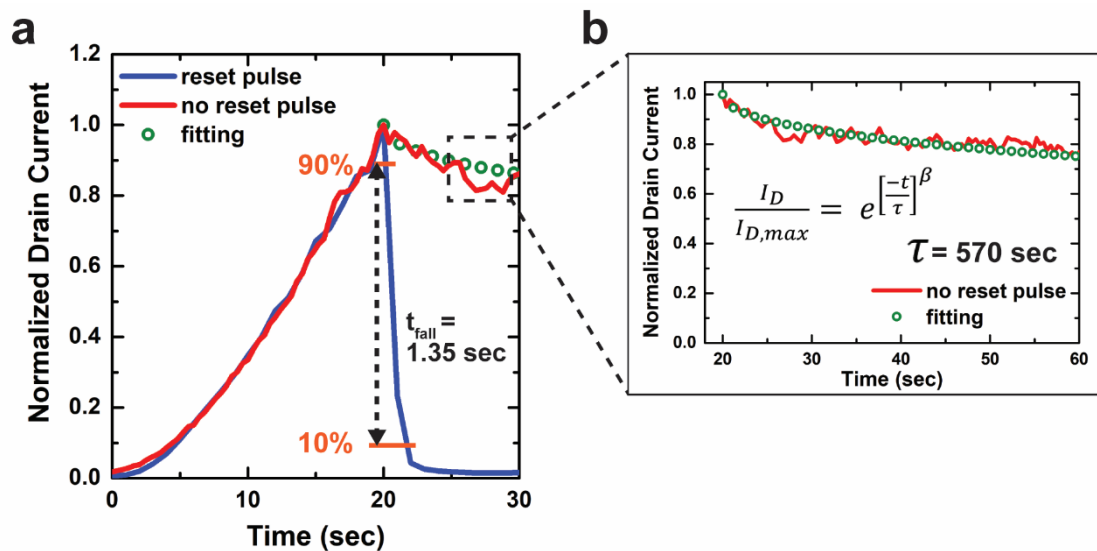
shows that the as-deposited ALD ZrO₂ thin film has at least one polycrystalline domain present.



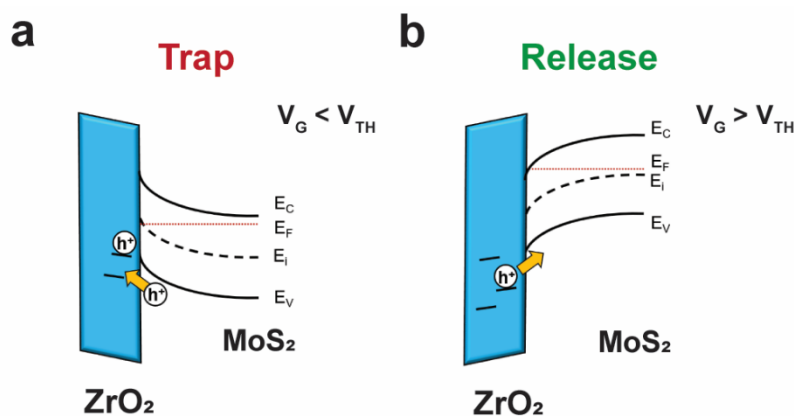
Supplementary Figure 10. Photoresponse of the gate current in (a) NCFG and (b) TiN-ZrO₂ device under green light illumination.



Supplementary Figure 11. Photocurrent as a function of the gate voltage at different optical power densities.



Supplementary Figure 12. Time response of the NCFG device under the application of a 20 second light pulse (optical power density of $10.35 \mu\text{W}/\text{cm}^2$) with $V_G = -150 \text{ mV}$ and $V_{DS} = 100 \text{ mV}$. (a) The red curve shows the intrinsic time response which displays the persistent photocurrent effect. The blue curve shows the improved fall time due to a 3 msec positive gate bias pulse. The green circle symbol line is the stretched exponential fitting to extract the time constant. (b) An extension of the persistent photocurrent decay and the stretched exponential fitting of the intrinsic time response. The extracted fitting parameters for β and τ were 0.47 and 570 seconds respectively.



Supplementary Figure 13. ZrO_2 trap/release mechanism overview based on gate biasing. (a) Under depletion mode gate biasing, photogenerated holes get trapped into ZrO_2 occupying oxide trap levels. (b) When applying a positive gate bias pulse, trapped charges are released.

References:

[1] V.K. Singh, B. Mazhari, AIP Advances, 2011, 1, 042123.

[2] J.-K. An, N.-K. Chung, J.-T. Kim, S.-H. Hahm, G. Lee, S. B. Lee, T. Lee, I.-S. Park, and J.-Y. Yun, Materials 2018, 11, 386.